Motion of a Solid Particle in a Water Flow Inside a Pipe

Salah Zouaoui, Aomar Ait Aider, Hassane Djebouri, Kamal Mohammedi, and Sofiane Khelladi

1 Introduction

Two-phase solid-fluid flow is occurring in various industrial and natural applications. Recently, several firms launched subsea mining projects because of an increasing demand on mineral materials from emerging countries. The knowledge of the behavior of solid particles allows the treatment and improvement of several industrial processes in the field of engineering processes such as drying, mixing, and separation.

Furthermore, transporting arbitrarily shaped particles is also of great importance in many biomedical applications. Namely, particles of various shapes such as spheres, disks, and rods have been developed for controlling and improving the systemic administration of therapeutic and contrast agents.

The idea considering bed load transport not as the flux of a continuous phase but as the superposition of the motion of individual particles has gained new attention from Böhm (2005). This approach has been without any doubt driven by the fast development of computing performances, enabling to solve numerically the equations of particle motion in interaction with the flow. Modeling phenomena that occur in this type of transport need more development and assessment of theoretical

S. Zouaoui • A. Ait Aider (✉) • H. Djebouri
Université Mouloud Mammeri de Tizi-Ouzou, Laboratoire de Mécanique Structure et Energétique (LMSE), 15000 Tizi Ouzou, Algeria
e-mail: zouaoui_salah2003@yahoo.fr; aitaider@yahoo.com

K. Mohammedi
Université M'hamed Bougara Boumerdès, Laboratoire d'Energétique Mécanique et Ingénierie (LEMI), MESOnexusteam, Boumerdès 35000, Algeria

S. Khelladi
Arts et Metiers ParisTech, DynFluid, 151 boulevard de l'Hôpital, 75013 Paris, France

F. Aloui, I. Dincer (eds.), *Exergy for A Better Environment and Improved Sustainability 1*, Green Energy and Technology,
https://doi.org/10.1007/978-3-319-62572-0_15

background. Particle motion is caused by a relative movement of the fluid and the forces to which the solid particle is subjected. The analysis of these phenomena requires mastering of the nature of the flow (laminar or turbulent), the evolution of potential interactions between the particles and especially the effect they induce on the change in physical properties of the flow (drag force, relative speed, etc.), and least but not last the influence of the transport properties of the surrounding medium on the prediction of particle trajectories.

In the context of subsea mining, the main task is to estimate the solid-liquid pressure drops in the flow line for various flow regimes.

In general, solid transport is divided into three major flow patterns: (1) pseudo-homogeneous flow (or homogeneous flow) and heterogeneous flow, (2) heterogeneous and sliding bed flow (or moving bed flow), and (3) saltation and stationary bed flow (Doron and Barnea 1996). Pseudo-homogeneous occurs when particles flow at very high velocities with a nearly uniform distribution in the pipe cross section. A decrease in particle flow rate induces the development of a heterogeneous flow pattern. A concentration gradient appears in the direction perpendicular to the pipe axis, with more particles transported at the lower part of the pipe cross section, as it is the case in most practical applications.

Solid transport in fluid flow is very complex, and most investigations focus on the determination of pressure gradients and critical deposition velocities in particle flows. The two-layer and three-layer models of the slurry flow were proposed by Doron et al. (1987) and Doron and Barnea (1993). Next, Wilson and Pugh (1988) put a forward dispersive-force modeling in heterogeneous slurry flow. But, the proposed models are not applicable to all solid types.

To carry large particles in vertical pipe, a predictive model is based on the work of Newitt et al. (1955) and Richardson and Zaki (1957). However, for horizontal pipe there are few models, and very large particle size has not been consistently explored (Ravelet et al. 2013).

To describe and study the behavior of a two-phase flow (liquid-solid) in a horizontal pipe, a test facility was built with a large particle injection system, and many tests have been carried. Flows were captured using a high-speed camera. Image-processing software was used to determine the flow characteristics such as particle trajectories and their state of motion (rest, rolling, or saltating motion).

Nomenclature

g	Gravitational constant ($m{\cdot}s^{-2}$)
$\vec{U}_p$	Vector velocity of particle ($m{\cdot}s^{-1}$)
$\vec{U}_f$	Vector velocity of fluid ($m{\cdot}s^{-1}$)
$\vec{F}_g$	Apparent weight of the particle (N)
$\vec{F}_m$	Force of the mass added to the particle (N)
$\vec{F}_{Basset}$	Basset force (N)
$\vec{F}_l$	Lift force (N)
$\vec{F}_{af}$	Acceleration force of the fluid (N)

(continued)

$\vec{F}_D$	Drag force (N)
C	Friction coefficient/concentration
C_d	Drag coefficient
C_l	Lift coefficient
C_m	Added mass coefficient
d_p	Particle diameter (m)
H_m	Average jump height (m)
L_m	Average length of jumps(m)
m_f	Mass of fluid (kg)
m_f	Mass of particle (kg)
Q_f	Volumetric flow rates of the liquid (l/s)
Q_s	Volumetric flow rates of the solids (l/s)
R_p	Particle radius (m)
S	Cross-sectional area of the pipe (m^2)
V_m	Mixture velocity (m/s)
V_c	Critical velocity
ΔP	Pressure drop (Pa)
Greek letters	
υ	Kinematic viscosity of fluid ($m^2 \cdot s^{-1}$)
ρ_f	Density of fluid ($kg \cdot m^{-3}$)
ρ_p	Density of the particle ($kg \cdot m^{-3}$)
$\vec{\Omega}$	Angular velocity of the particle ($rd \cdot s^{-1}$)
λ	Pressure drop coefficient

2 Description of Experimental Setup

2.1 Test Loop

We performed series of tests with the experimental loop shown in Fig. 1, for various materials that are described below. We focused our research on the liquid-solid particle flow in a horizontal rigid pipe of length $L = 2 \times 2$ m and diameter $D = 25$ mm. This tube carries a 180° horizontal curve with 30 cm diameter curvature. A pump (*salmson mark*) supplies the circuit with clear water. We made an injection system of the solid particles, and the particles fall down by gravity through a flexible tube connecting the bottom of the particle tank to the conduct via a buffer zone. The grain flow rate is adjusted by using a ball valve, and the mixture arrives in a system which is designed to separate the solid from the liquid. This system consists of a first tank provided with a filter, to recover the solid particles and allow only water to pass in a second tank. In order to realize a closed circuit for water, the second tank is connected to a pump which delivers the water into the circuit (Fig. 1).

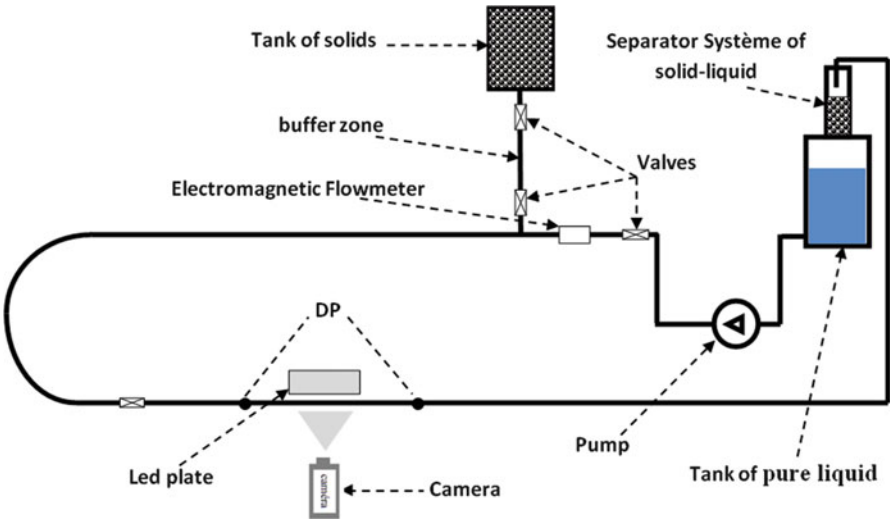

Fig. 1 Sketch of the test loop

2.2 Control Parameters and Measured Quantities

Measuring devices are used to obtain the flow parameters. The water flow rate is measured by an electromagnetic flowmeter (KROHNE Optiflux 2000) and adjusted by using a pump variator. The flow rate of solids is controlled by a device designed and manufactured in the laboratory. Optical measurements are also performed with a high-speed camera (Optronis CamRecord600), typically 1000 images are recorded with a resolution of 1280 × 1024 pixels at a frame rate of 500 Hz, and the flow is illuminated backward with a LED plate from Phlox.

2.3 Particles and Pipe

The experimental loop consists of a Plexiglas tube to visualize the solid/liquid flow. The estimated rugosity is 20 μm. Calibrated beads of alumina (Umicore, Alumina Degussit 92%, with a relative size dispersion of 10%) are used (Ravelet et al. 2013). The particles are relatively large, with sizes 60% of the pipe diameter. The physical and geometrical characteristics are summarized in Fig. 2.

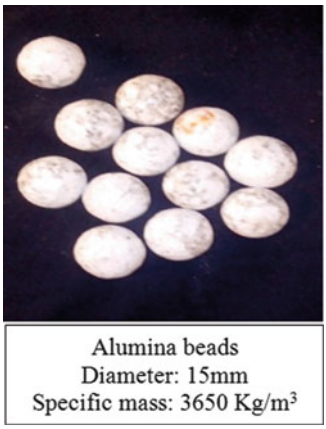

Fig. 2 Physical characteristics of the calibrated beads

3 Images Processing

The diagram in Fig. 3 shows the main processing steps, where the images are recorded by the CCD camera and saved in a "BMP" format. A Matlab program is elaborated for image processing.

To detect the particle positions, we used the CCD-captured images (Fig. 4).

4 Mathematical Modeling

The forces exerted on a solid spherical particle shape moving in a liquid are as follows:

4.1 Buoyant Force

The net weight of the particle and the buoyancy is given by

$$\vec{F}_{\mathrm{g}} = \left(m_{\mathrm{p}} - m_{\mathrm{f}}\right)\vec{g}, \tag{1}$$

4.2 Added Mass Force

A force created when one of the phases is accelerated:

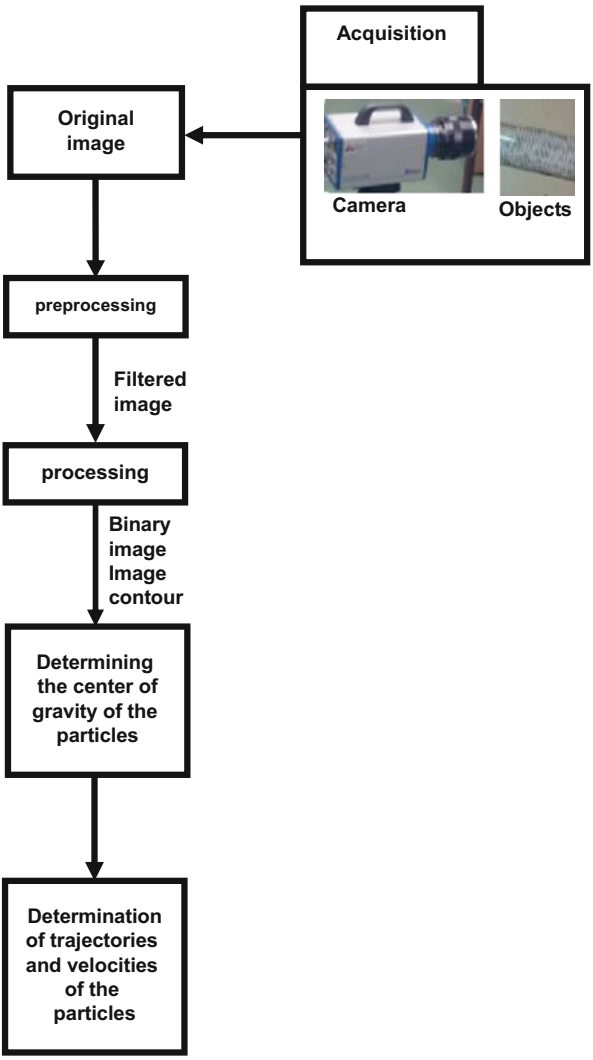

Fig. 3 The main processing steps

$$\vec{F}_{\mathrm{m}} = m_{\mathrm{f}} C_{\mathrm{m}} \frac{d\left(\vec{U}_{\mathrm{f}} - \vec{U}_{\mathrm{p}}\right)}{dt}, \tag{2}$$

4.3 Basset History Force

A force due to the effect of the fluid viscosity indicates the resistance to the particle movement at time t which depends on what happened before and can be written as

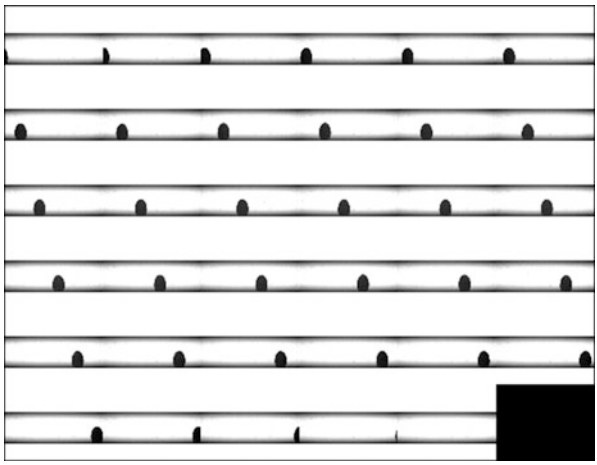

Fig. 4 Detection of the particle position from original images

$$\vec{F}_{\text{Basset}} = \frac{3}{2} d_{\text{p}}^2 \rho_{\text{f}} \sqrt{\pi \nu} \int_{-\infty}^{t} \frac{d\left(\vec{U}_{\text{f}} - \vec{U}_{\text{p}}\right)}{dx} \frac{dT}{\sqrt{t - T}}, \tag{3}$$

4.4 Magnus Force

A force due to the particle rotation is given by

$$\vec{F}_{\text{Magnus}} = \rho_{\text{p}} \left| \vec{U}_{\text{f}} - \vec{U}_{\text{p}} \right| \left(\Omega - \frac{1}{2} \frac{\partial U_f}{\partial z} \right) \vec{u}_{\text{z}}, \tag{4}$$

4.5 Drag Force

The following aerodynamic drag force correlation (Brown and Lawler 2003; Clift et al. 2005; Flemmer and Banks 1986) is used:

$$\vec{F}_{\text{D}} = -\frac{1}{2} \rho_{\text{f}} \pi \frac{d_{\text{p}}^2}{4} C_{\text{d}} \left| \vec{U}_{\text{p}} - \vec{U}_{\text{f}} \right| \left(\vec{U}_{\text{p}} - \vec{U}_{\text{f}} \right) \ , \tag{5}$$

In a fully turbulent regime, the drag coefficient C_d is independent of the particle velocity and Reynolds number (Peker and Helvaci 2011). Furthermore, a best approximation of the drag coefficient is $C_d \approx 0.44$.

4.6 Lift Force

A set of pressure gradients or shear forces are exerted on a fluid element as a consequence of a velocity gradient between the particles and the fluid:

$$\vec{F}_l = -\frac{1}{2}\rho_f \pi \frac{d_p^2}{4} C_l \left(U_T^2 - U_B^2\right) \vec{n} \ , \tag{6}$$

For high bubble Reynolds number *(Re_b)*, Auton et al. (1988) found that the lift coefficient (C_l) is independent on the Reynolds number and is equal to $\frac{1}{2}$. Magnaudet and Legendre (1998) have considered some transient effects of the lift force. They have showed analytically that just after the introduction of the particle in the flow, the lift coefficient is equal to $0.75\frac{3}{4}$ for any Re_b.

4.7 Force due to the Acceleration of the Fluid

The force induced by the fluid acceleration is given by the following expression:

$$\vec{F}_{af} = \rho_f \frac{4}{3}\pi R^3 \frac{d\vec{U}_f}{dt}, \tag{7}$$

From Newton's second law (FPD), the balance of forces exerted on a solid spherical particle moving in a liquid is

$$\begin{aligned} m_p \frac{d\vec{U}_p}{dt} = \vec{F}_g + \vec{F}_m + \vec{F}_{Basset} + \vec{F}_{Magnus}, \\ + \vec{F}_d + \vec{F}_l + \vec{F}_{af} \end{aligned} \tag{8}$$

Thus, for each force, the challenge is either to derive an appropriate description or to justify that it can be neglected. The description of the particle's motion is based on the mathematical and numerical resolution of Eq. (8). This resolution takes into account some simplifying hypotheses. Due to the existence of a large number of particles dispersed in the fluid, Basset force is neglected. The Magnus force is also neglected because the solid particle does not rotate on itself and is isolated in the flow (absence of interactions between particles). So, the dynamic equation becomes

$$m_{\mathrm{p}}\frac{d\vec{U}_{\mathrm{p}}}{dt} = \vec{F}_{\mathrm{g}} + \vec{F}_{\mathrm{m}} + \vec{F}_{d} + \vec{F}_{\mathrm{l}} + \vec{F}_{\mathrm{af}}, \tag{9}$$

4.8 Horizontal Pipe

Figure 5 shows the experimental and modeled trajectories of the solid particles for four different water volume flow rates which are 0.41, 0.67, 1.09, and 1.14 l/s.

These Figs. 5 and 6 bring several remarks:

- For water volume flow rate $Q_{ve} = 0.41$ l/s, we have seen that the solid particle rolls without slipping on the lower wall of the pipe. This phenomenon is due to the particle's weights. The results obtained for this case showed that experimental and modeled trajectories are almost identical. For a flow rate slightly larger than the first ($Q_{ve} = 0.67$ l/s), the particle leaves the bottom wall of the pipe and performs small bounces. From $x = 5$ cm, the bounces diminish gradually, and the particles settle over the bottom wall to adapt the phenomenon of rolling without slipping. The modeled path does not show particle jumps as the experimental case.
- At relatively high flow rates ($Q_{ve} = 1.09$ l/s and $Q_{ve} = 1.14$ l/s), the solid particle has a parabolic trajectory in both experimental and modeling cases. Length and height jumps are more important for Qve = 1.14 l/s.

4.9 Inclined Pipe

In this second case, we are interested in the effect of the slope on the jumps for a fluid velocity $U_{\mathrm{f}} = 0.41\ m/s$. The results, giving the average length and height of jump according to the speed of the fluid, are reported in Figs. 7 and 8.

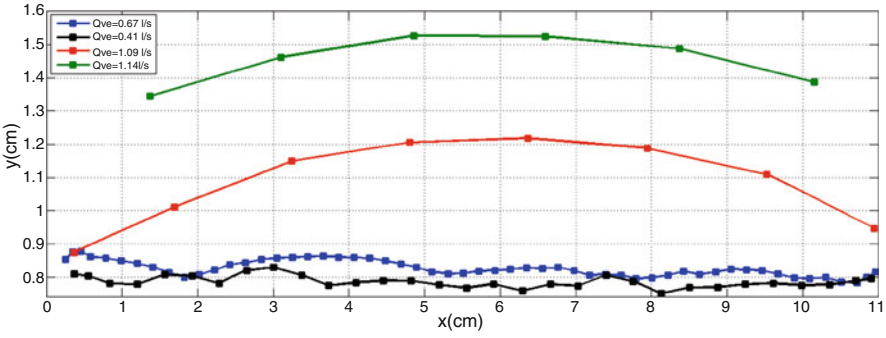

Fig. 5 Experimental trajectories of the solid particles for the different fluid volume flow rates

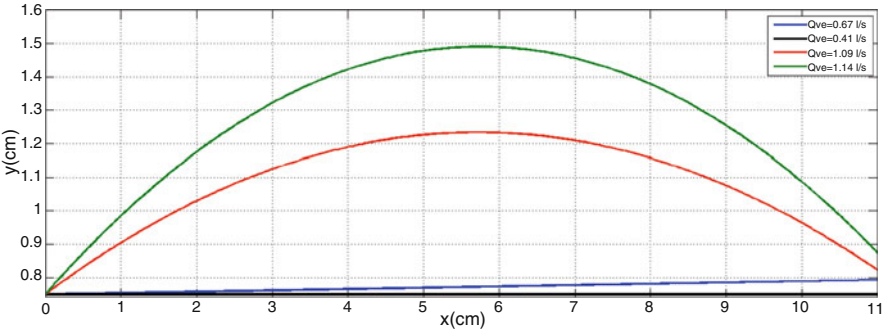

Fig. 6 Numerical trajectories of the solid particles for the different fluid volume flow rates

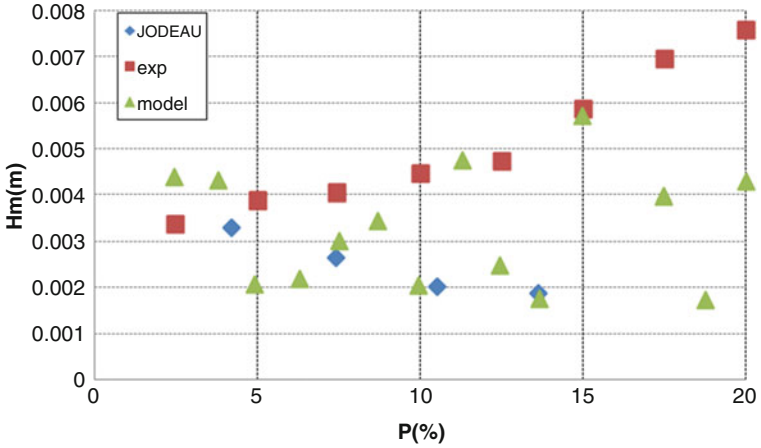

Fig. 7 The average height jumps versus the slope

From Fig. 7, we see that the jump height does not significantly depend on the slope; it varies between 0.002 and 0.004 mm. Figure 8 indicates that the length of the jumps increases with the increase of the slope for the experimental cases. In contrast, in our model, the length increases weakly; it is almost constant. This divergence in lengths can be explained by the effect of the free surface for the case of experience of Jodeau (2004), and the model is too simplified.

5 Pressure Drop in a Horizontal Pipe

Many mathematical models have been developed in order to predict the head losses in slurry transport. The most cited models are those of Durand and Condolios (1952) and Durand (1953); Worster and Denny (1955), Newitt et al. (1955), Gibert

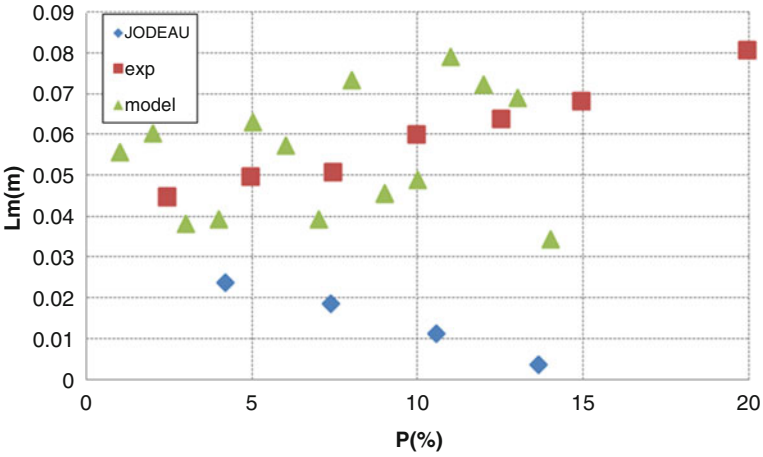

Fig. 8 The average length of the jumps versus the slope

(1960), Fuhrboter (1961), Jufin and Lopatin (1966), Zandi and Govatos (1967), and Zandi (1971); Turian and Yuan (1977), Doron et al. (1987), Bank et al. (1989) and Doron and Barnea (1993); and Wilson et al. (1992), Matousek (1997), Bratland (2010), and Ravelet et al. (2013). Some models are based on phenomenological relations and, thus, result in semiempirical relations; others tried to create models based on physics, like the two- and three-layer models.

The aim of the present section is to measure the pressure drops in different parts of the test loop as a function of solid concentration and mixture velocity. The parameters that are adjusted with experimental means are the volumetric flow rates of the liquid (Q_l) and of the solids (Q_s). The following set of parameters is chosen for presenting the results. The first is the mixture velocity (V_m), and the second is the delivered concentration (C):

$$V_m = \frac{Q_l + Q_s}{S}, \tag{10}$$

$$C = \frac{Q_s}{Q_s + Q_l}, \tag{11}$$

where S is the cross-sectional area of the pipe. This mixture velocity is a volumetric average of the velocities of each phase. The pressure drop is measured using two differential pressure sensors (VEGADIF65).

If the particle starts building up in the pipe, this implies that the pressure and friction loss also increases depending on the mixture velocity of the flow. It is important to assess how these solids might affect the gradient of pressure. The thick black line in Fig. 9 stands for the measured pressure gradient for water flowing alone. When there is no particle ($C = 0\%$) in the pipe, the friction loss starts increasing quadratically with the velocity of the mixture. The curve is a fit of the

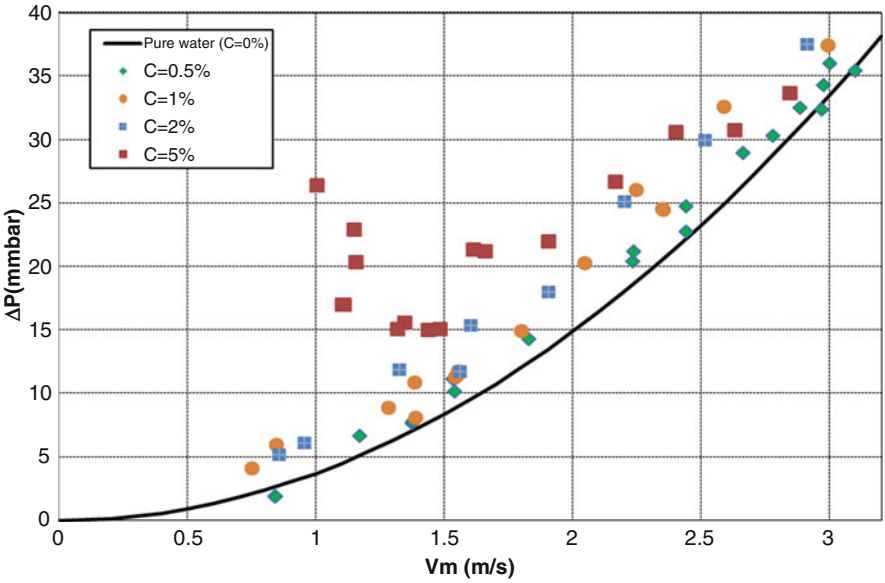

Fig. 9 Pressure drop ΔP vs. mixture velocity V_{m}

form $\Delta P = \frac{\lambda}{D} \cdot \frac{\rho V_{\mathrm{m}}^2}{2} \cdot L$, where $L = 1.4$ m and λ is calculated by Colebrook formula.

With particles (at $C = 0.5$, 1 and 2%) flowing in the pipe, the friction loss is higher even though the particles are carried by the fluid. The pressure drop increases dramatically when high flow rates are exhibited as shown in Fig. 9. The pressure drop curves behave as the clear-water pressure drop curve and follow the same trend.

At $C = 5\%$, the solid-liquid curve in Fig. 9 shows how the pressure drop decreases with the reduction of the flow velocity. At this region, some particles can accumulate at the lower section of the pipe, and the rest keep circulating. However, if the mixture velocity keeps decreasing, there is a high probability that the particle buildup increases, and as a result the pressure drop increases again. The main idea is basically to maintain a balance in the velocity to avoid the pipe blocking and the high pressure drop. The shape of the pressure drop curve does not vary monotonically with the velocity. Following the definition of Doron et al. (1987), the mixture velocity which corresponds to the minimum hydraulic gradient is called critical velocity (V_{c}). In the present case, the critical velocity is $V_{\mathrm{c}} \simeq 1.48$ m/s.

6 Conclusions and Future Work

This work focused on modeling, simulating, and experimenting the transportation of solid particles in a fluid flow inside a pipe. Little work has been done in this area. Two main objectives were set in the present work:

- Experimental and modeling study of the trajectories of solid particles on independent jumps in horizontal and inclined pipe
- Experimental study of hydraulic transport of large particles in horizontal pipe

The results obtained for particle trajectories were analyzed in order to understand the mechanisms of the solid transport. Modeled trajectories are compared with experimental results. These results highlight the effect of the water speed on the trajectories.

The hydraulic gradient as a function of mixture velocity has been measured for calibrated beads of specific mass equal to 3650 $kg.m^{-3}$, with large particle-to-pipe diameter ratio up to 60%. Tests have been conducted in a horizontal pipe. The main results are the following:

- For $C = 0.5$–2%, the pressure drop increases slightly, and its curves behave as the clear-water pressure drop curve and follow the same trend. All particles are carried by the fluid.
- For $C = 5\%$, the pressure drop is higher comparatively to the case without solid.
- For $V_m < V_c$, we observed flow regimes with a stationary bed above which a compact layer of beads is flowing. Therefore, the pressure drop becomes very important.
- When speed increases ($V_m > V_c$), the particles are held in suspension, and pressure drop curves follow the trend of clear-water curve.

Other sets of tests are needed to extend this study to other configurations with other types of particles.

As part of this work, a method for simulating the transport of solids in a Newtonian fluid has been developed in collaboration with the Laboratory of Fluid Dynamics (DynFluid) at Arts et Métiers ParisTech high school. This method is based on the volumes of fluid with penalty. The fluid behavior is governed by the Stokes equations and then is extended to the Navier-Stokes equations within the investigation domain. The motion of rigid particles is governed by the fundamental principle of dynamics, while fluid/structure coupling is managed by a penalty method. The validation step of the theoretical work is done through experimental battery of tests.

Acknowledgments This research was supported by the DynFluid Laboratory at Arts et Métiers ParisTech. We would like to express our gratitude to Pr. Farid BAKIR for his assistance in the design and development of the experiment.

References

Auton, T.R., Hunt, J.C.R., Prud'Homme, M.: The force exerted on a body in inviscid unsteady non-uniform rotational flow. J. Fluid Mech. **197**, 241–257 (1988)

Bank, R., Welfert, B., Yserentant, H.: A class of iterative methods for solving saddle point problems. Numer. Math. **666**, 645–666 (1989)

Böhm, T.: Motion and interaction of a set of particles in a supercritical flow. Thesis, l'Université Grenoble 1 – Joseph Fourier (2005)

Bratland, O.: Pipe flow 2: multi-phase flow assurance (2010)

Brown, P., Lawler, D.: Sphere drag and settling velocity revisited. J. Environ. Eng. **129**(3), 222–231 (2003)

Clift, R., Grace, J.R., Weber, M.E.: Bubbles, Drops, and Particles. Dover Publications, Inc., Mineola, New York, USA (2005). ISBN: 0-486-44580-1

Doron, P., Barnea, D.: A three layer model for solid liquid flow in horizontal pipes. Int. J. Multiphase Flow. **19**(6), 1029–1043 (1993)

Doron, P., Barnea, D.: Flow pattern maps for solid–liquid flow in pipes. Int. J. Multiphase Flow. **22**, 273–283 (1996)

Doron, P., Granica, D., Barnea, D.: Slurry flow in horizontal pipes, experimental and modeling. Int. J. Multiphase Flow. **13**(4), 535–547 (1987)

Durand, R.: Basic relationships of the transportation of solids in pipes – experimental research. Proceedings of the International Association of Hydraulic Research, Minneapolis (1953)

Durand, R., Condolios, E.: Etude experimentale du refoulement des materieaux en conduites en particulier des produits de dragage et des schlamms. Deuxiemes Journees de l'Hydraulique. 27–55 (1952)

Flemmer, R., Banks, C.: On the drag coefficient of a sphere. Powder Technol. **48**(3), 217–221 (1986)

Fuhrboter, A.: Über die Förderung von Sand-Wasser-Gemischen in Rohrleitungen. Mitteilungen des Franzius-Instituts, H. 19 (1961)

Gibert, R.: Transport hydraulique et refoulement des mixtures en conduites. Annales des Ponts et Chausees. **130**(3), 307–374 (1960.), **130**(4), 437–494

Jodeau, M.: "Etude expérimentale des mécanismes de transport solide par charriage torrentiel". Mémoire de DEA, Cemagref Grenoble Février (Septembre 2004)

Jufin, A.P., Lopatin, N.A.: O projekte TUiN na gidrotransport zernistych materialov po stalnym truboprovodam. Gidrotechniceskoe Strojitelstvo. **9**, 49–52 (1966)

Magnaudet, J., Legendre, D.: Some aspects of the lift force on a spherical bubble. In: Fascination of Fluid Dynamics, pp. 441–461. Springer Netherlands, Dordrecht (1998)

Matousek, V.: Flow mechanism of sand/water mixtures in pipelines. PhD thesis, Delft University of Technology, Delft (1997)

Newitt, D.M., Richardson, M.C., Abbott, M., Turtle, R.B.: Hydraulic conveying of solids in horizontal pipes. Trans. Inst. Chem. Eng. **33**, 93–110 (1955)

Peker, S.M., Helvaci. S.S.: Solid-Liquid Two Phase Flow. Elsevier Science (2011)

Ravelet, F., Bakir, F., Khelladi, S., Rey, R.: Experimental study of hydraulic transport of large particles in horizontal pipes. Exp. Thermal Fluid Sci. **45**, 87–197 (2013)

Richardson, J.F., Zaki, W.N.: Sedimentation and fluidisation. Trans. Inst. Chem. Eng. **32**, 35–53 (1957)

Turian, R.M., Yuan, T.F.: Flow of slurries in pipelines. AICHE J. **23**, 232–243 (1977)

Wilson, K.C., Pugh, F.J.: Dispersive-force modeling of turbulent suspension in heterogeneous slurry flow. Can. J. Chem. Eng. **66**, 721–727 (1988)

Wilson, K.C., Addie, G.R., Clift, R.: Slurry Transport Using Centrifugal Pumps. Elsevier Applied Sciences, New York (1992)
Worster, R.C., Denny, D.F.: Hydraulic transport of solid materials in pipelines. Inst. Mech. Eng. (London). 563–586 (1955)
Zandi, I.: Hydraulic transport of bulky materials. In: Zandi, I. (ed.) Advances in Solid–Liquid Flow in Pipes and Its Applications, pp. 1–38. Pergamon Press, Oxford (1971)
Zandi, I., Govatos, G.: Heterogeneous flow of solids in pipelines. Proc. ACSE J. Hydraul. Div. **93** (HY3), 145–159 (1967)